Biocybernetics and Biomedical Engineering
2010, Volume 30, Number 3, pp. 49–64

Image Processing Algorithm for Cell Force Sensor with a Micropillar Patterned Substrate

WALDEMAR T. SMOLIK[1,*] , WOJCIECH ŚWIĘSZKOWSKI[1], KRZYSZTOF J. KURZYDŁOWSKI[1], ARIE BRUININK[2], NORBERT DANZ[3]

[1] *Warsaw University of Technology, Warsaw, Poland*
[2] *Empa. Swiss Federal Laboratories for Materials Testing and Research, St. Gallen, Switzerland*
[3] *Fraunhofer Institute for Applied Optics and Precision Engineering, Jena, Germany*

The paper presents an image analysis for cell force measurement using a patterned substrate surface. The cell forces are transduced to a hexagonal lattice of microcantilevers in the shape of cylindrical pillars installed on a substrate surface. The magnitude and direction of pillars deflection is measured optically by an analysis of transmission images of the substrate. The template matching is used for identification of the position of pillars. The hexagonal lattice of pillars is identified automatically and used as information about the reference rest position of the pillars. The elaborated algorithm was tested using simulated data. The first results using real images are presented.

K e y w o r d s: cell forces, cell motility, cell imaging, micro-patterned substrate, micropost array, image processing

1. Introduction

Cell migration and motility plays a critical role in many physiological processes that depend on dislocation of the cells such as embryonic development, tissue regeneration and homeostasis as well as immune reactions. An accurate understanding of mechanical basis of generation of force responsible for cell migration is very important for understanding the cell behavior [1, 2] and functional state of the cell. Therefore it may be significant for fundamental and applied biological research in the direction of pharma/toxicodynamics, drug effects, cancer therapy, wound healing including scar, osteoporosis therapy, etc.

* Correspondence to: Waldemar T. Smolik, Warsaw University of Technology, ul. Nowowiejska 15/19, 00-665 Warsaw, Poland, e-mail: W.Smolik@ire.pw.edu.pl
Received 4 September 2009; accepted 8 March 2010

Cell transduces traction forces to external surfaces being in most cases the extracellular matrix (ECM) through the cytoskeleton – the mesh of protein fibers within the cytoplasm. The cytoskeleton consisting of microtubule, actin and other fibres defines the cell shape, enables motion (by structures such as flagella, cilia and lamellipodia). Size of traction forces for fibroblasts is described to be between 0.1 nN and 4.1 μN/cell [3, 4].

A number of methods have been developed to measure cell forces. The one of the first methods involves plating cells onto a thin layer of a flexible membrane [5]. Another approach involves embedding fluorescent beads into a polyacrylamide gel substrate [6]. Cells deform the substrate by applying traction forces and produce a wrinkled pattern on the substrate in the first method or deform the pattern of embedded beads in the gel. The recent version of this method doesn't provide quantitative data because the direct influence of local changes of the membrane on elasticity parameters in the neighbourhood leads to a very complex data analysis.

An alternative method of measuring of traction forces is the use of a microchip with a matrix of microcantilevers as substratum of moving cells [7–11]. The cantilevers bend in a response to cell forces. The cantilevers deviation from the rest position is taken as an index to quantify traction forces. The force calculation method is discrete in a sense that only forces in the orientation of the cantilevers are measured. A simple mechanical model of cantilever bending requires knowledge of a spring constant. A principal advantage is that the use of cantilevers does not require any complex mathematics as needed for the previous systems.

Our group participated in developing of a cell force sensor using the latter set-up (Fig. 1). A hexagonal grid of cylindrical micropillars was proposed as a substrate surface pattern. The hexagonal grid is optimal for a maximum surface of adhesion with a given inter pillar distance. The red light transmission image of a pillar matrix is registered in the designed device. The tops of cylindrical pillars appear as bright circles (spots) in the image. The tops of bent pillars are seen as circles shifted from nodes of a regular hexagonal grid (Fig. 2). The magnitude and direction of the shift give the information regarding the force vectors. The accuracy of force measure-

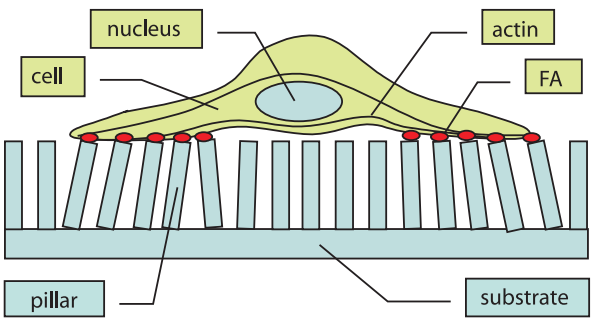

Fig. 1. Cell force sensor with pillared substrate (side view)

ments relies on automation and quality of the image analysis. Different methods were proposed in the literature [9, 12, 13] for image analysis.

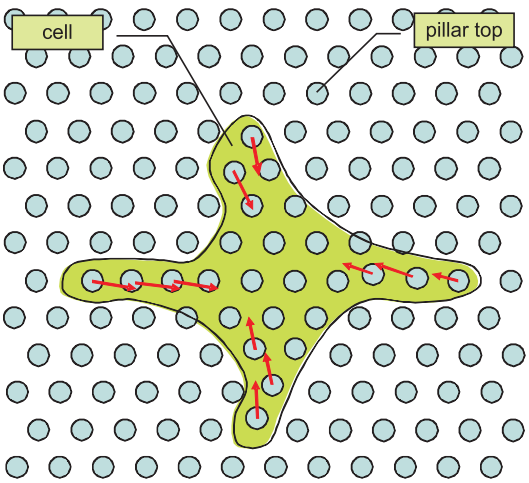

Fig. 2. Top view of the cell force sensor with the hexagonal grid of cylindrical cantilevers. Some pillars are shifted by the cell contraction forces (arrows)

This paper presents a dedicated to a hexagonal grid of pillars, semi automatic image processing algorithm for identification of the cell forces. The calculation of pillar bending requires information about the dislocation in comparison to the reference position. The different methods may be used to determine the reference position of pillars: 1) registration of an image of the pillar matrix without a cell culture, 2) a registration of an image of the bottom of pillars [9], 3) calculation of a reference grid using pillars unoccupied by cells (or unbent). In the first case, the registration of empty substrate requires preserving of the same position of pillar matrix before and after placing a cell culture on the substrate surface. The specialized procedure for a cells' placing or a substrate positioning has to be used. In the second case, the registration of the bottom of pillars requires much more complicated optical system. Because of these reasons the third method was selected for implementation. The automatic identification of hexagonal grid eliminates the need of the registration of any additional reference images.

2. Cell Force Sensor

The presented image analysis is dedicated to the CellForce optical device designed by the IOF Jena group. The biosensor is a complete imaging system for cells visu-

alization (Fig. 3). The optical system consist of light sources – colour light emitting diodes (red, green and blue), a system of lenses and prisms, the NeoFluar zoom objective with the piezo focus controller and the AVT Pike F421B monochrome CCD camera.

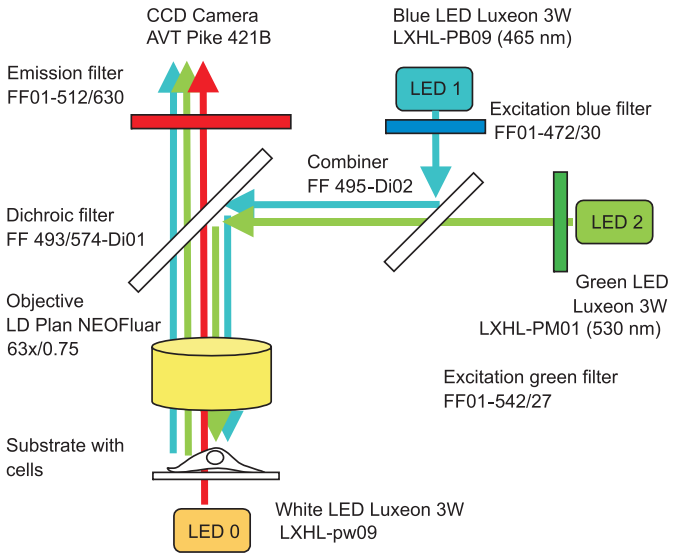

Fig. 3. Cell force sensor optics design

The LEDs used for pillar membrane illumination together with the system of prisms and lenses allow registration of transmission images of micropillars and fluorescent images of the cells. The cells are fluorescently labeled in order to monitor additionally the cell shape during the tests [14]. The transmission images of deflected pillars are registered using white color LED illuminating the bottom of the substrate. The pillars act as waveguides due to material transparency. The tops of pillars are imaged as circles in the picture. The red light (wavelength 800–900 nm) does not interact with the cells as well as with the fluorescence dyes. The fluorescence images of the cells are registered using green and blue colour LEDs that illuminate sequentially the cells from the top. The transmission and fluorescence images are registered using a high sensitivity, low noise CCD camera. The specialized microchamber is used for live cells. The chamber contains fluid connections that enable cultivation of the cells under the cell culture conditions during the measurements. The glass windows from the top and bottom enable the microstructure observation.

The micropillar matrix should meet several contradictory requirements on chemical, mechanical and optical properties. The material should be adhesive for the cells (only on the top of pillar), transparent to enable registration of the transmission images of pillar array, and may no manifest fluorescence in case of cell fluores-

cence imaging. The elastic modulus should be low enough that 10 to 100 nN force exerted by a cell will detectably bend the pillars. In the time of writing this paper, Elastollan® 1180A50 (polyether-based thermoplastic polyurethane) and Sylgard® 184 (polydimethylsiloxane) were selected for the tests.

The different surface modifications either with polyethylene glycol (PEG), hydroxylethyl methacrylate, hexamethylene diamine or chitosan applied using UV irradiation, gamma irradiation (GI) and interfacial modification (IM) were tested [15]. Finally, the pillar matrix was prepared from Elastollan®1180A50 by injection molding. The IM with PEG was used for the surface modification to increase the cell adhesion to the pillar tops. The sides of pillars were oxidized with hydrogen peroxide (H_2O_2) and then impregnated with PEG 400 to decrease the cell adhesion [16] and to prevent the migration of cells between pillars [17].

The basic set-up of the cell force sensor substrate is shown in Fig. 1. The substrate surface of 5 mm^2 is covered by the hexagonal grid of pillars. Each cylindrical pillar has a diameter of 5 μm corresponding to the size (1–5 μm) of a actin fibres focal adhesion dot [18]. The pillar dimensions and the distance between pillars depend on range of the cell forces and type of material used. The centre-to-centre distance equal 10 μm and 25 μm pillar height corresponds to material stiffness of a few dozen of nN/μm. The sensor array consists of 250,000 micropillars. Because of the large number of needed items the reproducibility and the high precision of the produced parts are a challenge. Cavities built by different manufacturing processes (silicon etching and UV-LIGA – UV-Lithography, galvano forming, replication) were tested by the IFAM group as moulds for the pillar array [19]. In order to manufacture these pillar arrays by micro-injection moulding a complex variotherm moulding process under vacuum with plasma coated inserts was developed.

3. Image Analysis

An appropriate numerical analysis needs to be applied to calculate the cell forces from the images of the patterned substrate (Fig. 4). A hexagonal grid of pillars dedicated, semi automatic image processing algorithm was elaborated. The following assumptions were taken for the image processing. The cells pass the contraction forces to the substrate surface with a known size hexagonal lattice of microcantilevers in the shape of cylindrical pillars. The pillar tops appear on transmission image of a substrate as spots (circles). The spots shifted from a grid nodes correspond to the pillars bent by the cell contraction forces. The software task is to identify the spots and calculate the direction and value of displacement vector of spots.

Information about base position of a pillar is required to calculate the pillar bending. A reference hexagonal grid is identified using pillars unoccupied (not deflected) by the cells. When the reference hexagonal grid is found i.e. rotation of three hexagonal axes, zero position and size of the grid are known; the rest position

of all pillars is calculated. Using the difference between the rest and bent positions of the pillar the force vector direction and value is calculated. The following image processing tasks are performed for identification of the pillar bending:

- identification of spots (tops of pillars) in the image,
- classification of pillars into two groups: bent and unbent by the cells,
- identification of reference hexagonal grid using not-shifted spots,
- calculation of spots' shift and calculation of force vectors.

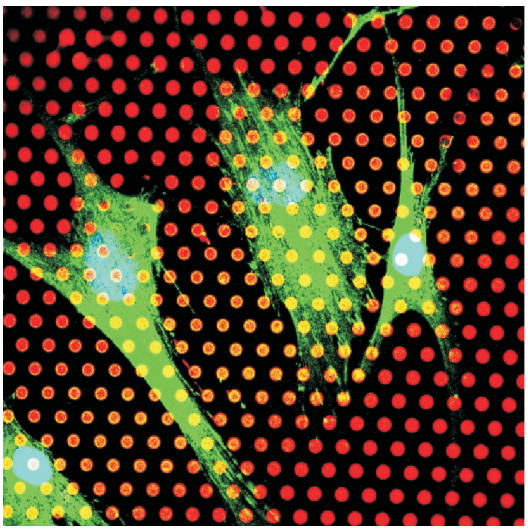

Fig. 4. Transmission image of the pillar substrate, green and blue fluorescent images of cells added as three color components of a RGB bitmap. 24 bits, 1024 × 1024 pixels. The pillar diameter is 5 μm. The inter pillar distance is 10 μm centre to centre

3.1. Identification of Spots (the Tops of Pillars)

The different types of pattern recognition algorithms were considered in respect to the pillar position identification. Among others the thresholding with morphological transformations and the template matching methods were tested [20]. The tests were performed on numerically simulated images and on real images. Many images were registered for tests using a confocal microscope and the elaborated CellForce sensor. It was turned out that the simulation does not take some systematic errors like pillar matrix deformation into consideration. The substrate material is not stiff thus the pillar matrix can be deformed in a process of the matrix removing from a mould. Due to non-uniform background illumination the pillars appear as bright or dark spots depending of their position in the image (Fig. 5). Thus, apart denoising additional preprocessing procedures are required: background elimination and morphological

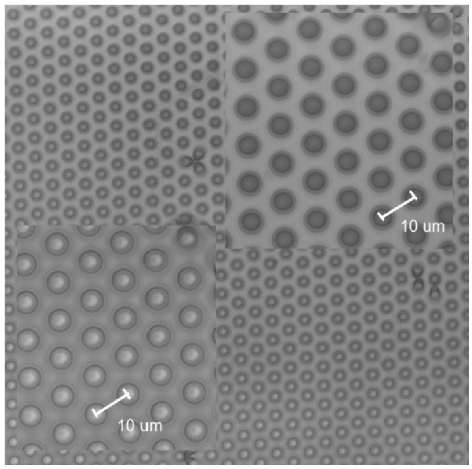

Fig. 5. Transmission image of the pillar flexible non-flat substrate. Bottom left and upper right corners are zoomed. Pillars appear as bright (bottom left) or dark (top right) spots due to non-uniform lighting

operations (erosion, dilation) to remove small artefacts and to correct shape of the pillar spots (Fig. 6).

For image denoising the averaging filter with 3x3 pixels window and the median filter with 5x5 pixels window is applied. Then, the morphological opening is performed in order to find the background illumination that may be non-uniform in the whole image. To remove the pillar spots the structuring element of a diameter greater than the know diameter of pillar is used. The subtraction of the background makes the image more uniform.

The next step is to perform the morphological opening again but at this time using a structuring element of circular shape and the diameter corresponding to the size of pillar. The small objects are removed and shape of the circles is restored. Then, the thresholding is performed using experimentally selected threshold level that generates the binary image. The eroding procedure is the next step to remove again small artefacts.

Since the size and shape of the searched objects are known a template matching algorithm – the Hough transform for circles [20] – was selected for identification of the spots. Because the existing source codes for the transform are dedicated to detection of circles of any size and are optimized for calculation speed at cost of accuracy, the own implementation of the Hough transform was elaborated for detection of circles of the known size. The convolution with two-dimensional kernel is calculated where the kernel is a circle or ring pattern. Two-dimensional accumulator is created and local maxima detection is performed. Because of differences in appearance of the pillars in the image, two versions of the Hough transform were implemented: for circles and for rings to overcome this problem.

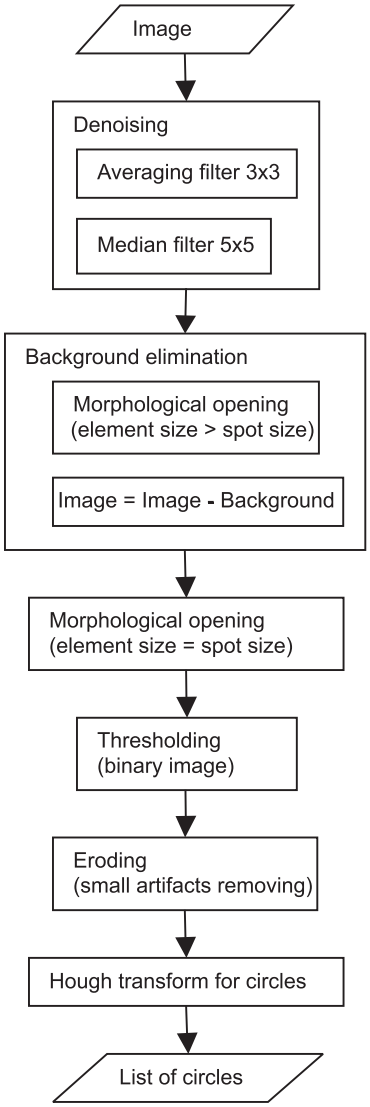

Fig. 6. Identification of spots

3.2. Classification of Spots

To find the reference position of hexagonal grid, the pillars unoccupied by the cells (not shifted spots) have to be identified. The first scenario of finding not bent pillars was to detect the cell contours in a fluorescence image and to exclude the pillars from these regions from the analysis. However, the fluorescence images are not easy to analyze because of a low signal to noise ratio, non-uniform dye distribution in cell

and not closed cell contours. The applied alternative method eliminates the need of the cell recognition. The neighborhood of each individual pillar is analyzed (Fig. 7). The known diameter and the inter pillar distance determine the size of neighbourhood. The six spots in a given distance range (Fig. 8) that compose a hexagonal structure are searched. The spots are sorted according to angular orientation and assigned to the directions shifted by 60 degrees. The structures with at least four neighbour spots are taken to the calculation. The three hexagon diagonals that correspond to the axes

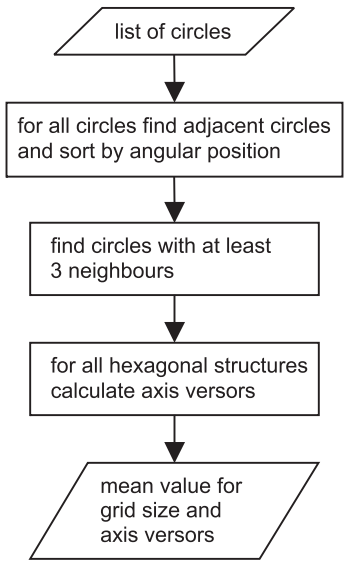

Fig. 7. Identification of hexagonal grid

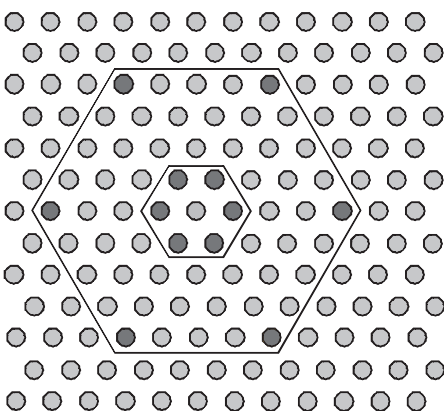

Fig. 8. Top view of pillar matrix. Six adjacent spots compose a hexagon. Six spots situated at given distance in the selected directions (grid axes) compose a larger hexagon

of hexagonal grid are calculated. The versors of hexagonal axes are calculated by averaging the data obtained for all hexagons. The procedure is repeated for the larger hexagon to increase the precision of the orientation calculation (Fig. 9).

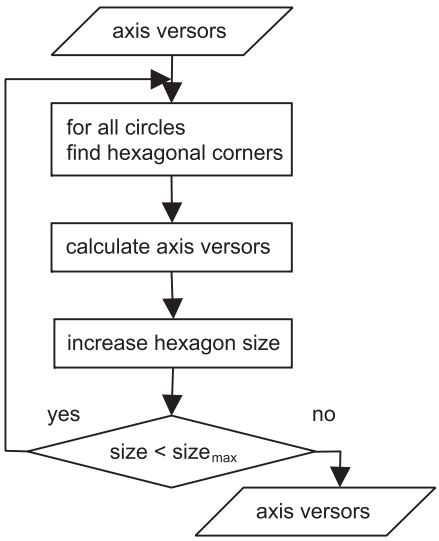

Fig. 9. Improvement of hexagonal axes identification

The automatic classification of the spots requires sometimes the intervention of the user. The user has possibility to draw the region of interest to mark the spots covered and bent by the cells.

3.3. Identification of a Reference Hexagonal Grid

The hexagonal grid identification is performed by a least square optimization. The least square norm is minimized by a linear search performed in a four-dimensional space with coordinates: rotation, (X,Y) position and grid size. The sum of the distances between the identified pillars and the corresponding grid nodes is used as a norm. For each pillar the nearest grid node is found using simple trigonometrical relationships. The distance for a few hundred pillars presented in the image is calculated very fast. The search is limited to a small range in each coordinate because approximately the grid size is known, the grid rotation is found by the analysis of spots in the direct neighbourhood and the search in the position coordinates is limited to the size of a node. The grid fitting is performed in a few steps (Fig. 10) to increase quality of the fit. The shifted pillars that don't fit to the regular grid with given tolerance are excluded and the fitting is repeated. In this way the pillars bent by the cells are excluded from the analysis. The method eliminates need of the cell recognition and finds the

bent pillars itself and eliminates them from calculating the position of a reference hexagonal grid. Not only the pillars covered by the cells but also the pillars deformed during the moulding process are excluded from the calculations.

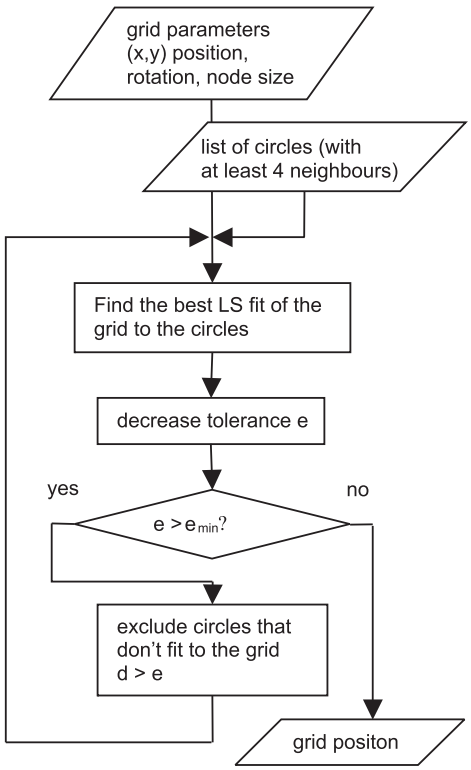

Fig. 10. Fitting of hexagonal grid

The described algorithm performed well for simulated data even for an image with high noise but the grid fitting for real data was weak. The procedure fitted well the grid in the image centre but poorly in the corners. The reason of this is that the pillar matrix made of flexible polymer material can be stretched or squeezed on the edges in the process of mould removing. The algorithm was enhanced to perform a fit to an irregular grid. The spots are assigned to the lines of the reference grid calculated in the previous step. Every line of the hexagonal grid is fitted to the appropriate row of the pillar spots using a linear regression procedure. The grid nodes are calculated as a cross-section of three lines (a point with minimum distance to these three lines). Finally, the fitting procedure assigns each spot to the node of the reference grid. The tests on real images showed that the enhanced algorithm performed well also for irregular grid.

3.4. Calculation of Force Vectors

The semi-automatic image processing was elaborated and implemented in the MATLAB environment as the CellForce script toolbox. The images are loaded as 24-bit true color bitmaps. The RGB colour components are used to store the transmission image of substrate with pillar matrix (red) and the fluorescent images of cells (green, blue). First, the image preprocessing i.e. denoising, background elimination and morphological operations are performed. The circular spots are identified using the Hough transform for circles or rings depending on selected option. The parameters like a dilation coefficient, geometrical parameters of the pillar matrix, a distance between the pillars, a pillar diameter and a threshold level for local maxima detection are selected by the user. The tolerance coefficients have an influence on the quality of classification of the spots to bent or unbent pillar group. The user has a possibility to add pillar positions not detected by the automatic algorithm or to remove false detected pillars. After the identification of the reference grid the force vectors are calculated and displayed.

The vectors of spot displacements are calculated with a reference to the grid nodes. The force value is calculated using mechanical and geometrical parameters of the pillars. The pillar deflection, in a linear range of deformation, is proportional to the focal force applied by the cell [17]. The force is calculated using formula:

$$F = \frac{3}{4}\pi E \frac{r^4}{L^3}\Delta x \tag{1}$$

where r, L, and Δx are the radius, length and deflection of the pillar respectively, and E is the Young's modulus.

4. Verification of the Algorithm and Results of Image Analysis

To verify the elaborated algorithm the images with pillar hexagonal matrix and elliptic shape cell-like objects were numerically simulated. The simulation procedure allows to setup several parameters of a pillar hexagonal grid, pillar properties, image and noise characteristics. The cell-like object is described by a position, rotation and size of ellipse, and by pillar bending function $f(r,\alpha,t)$. The $f(r,\alpha,t)$ function describes deflection of the pillars in the elliptic region where (r,α) are polar coordinates relative to the centre of the ellipse and t is time. The cell contraction or expansion can be simulated using linear or square function. The Gaussian noise was added to a post position and pixels value. The simulated data are stored in the true colour, 24-bit bitmap format as two separate RGB components. The pillar matrix is stored in the red channel and cell-like object in the green channel. The blue channel is used to store vector graphics presenting the bending forces.

Figure 11 shows example results of the elaborated image processing algorithm for numerically simulated data. In the simulation the elliptical cell-like object contracts i.e. the bending forces are oriented to the centre of an ellipse. The pillar grid is malformed (stretched) on the edges. The spots are well identified on the simulated noisy image (Fig. 11a). The regular grid well fits to the pillar spots in the image centre but not near the edges (Fig. 11b). The enhanced algorithm fits irregular grid in the centre as well as near the edges (Fig. 11c). The detected force vectors are presented in Fig. 11d. The scale of 100 nN is drawn in bottom left corner of the image. The procedure achieved good results for the simulated, free of noise images as well as for noisy images.

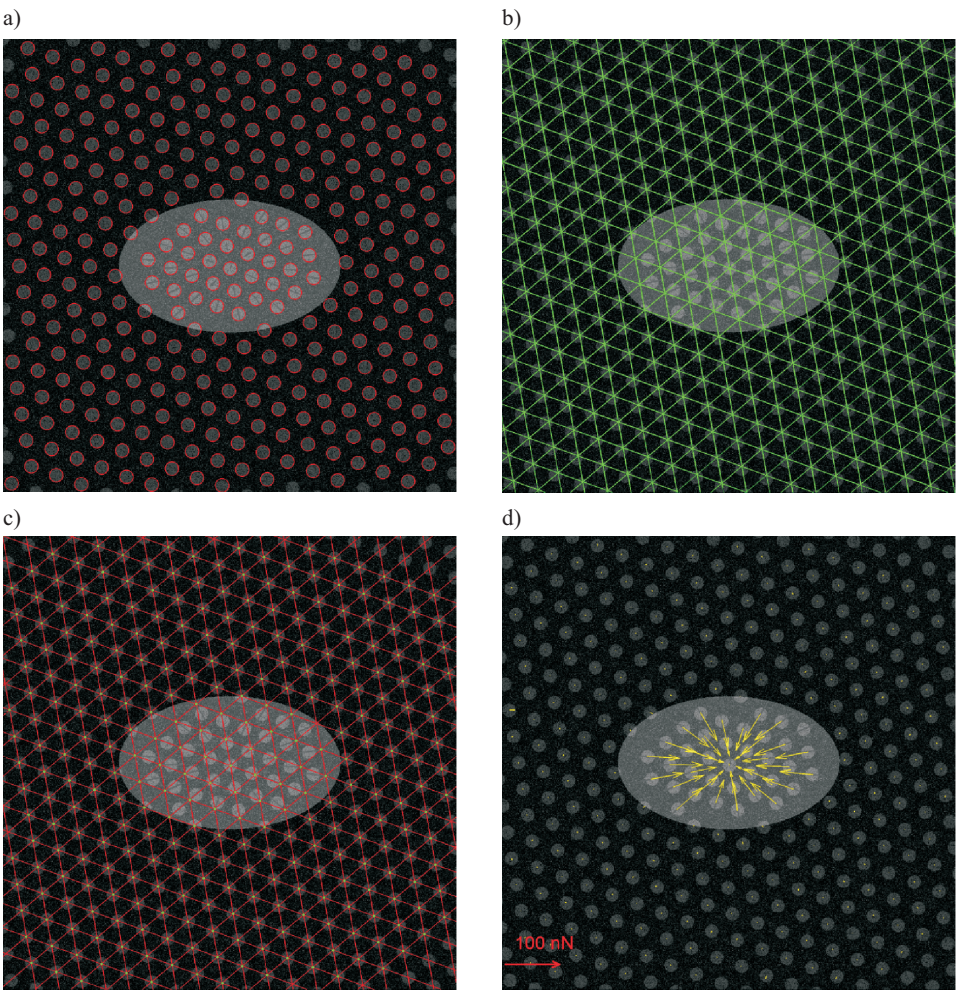

Fig. 11. Image processing of simulated contracting object (added Gaussian noise). a) Identified pillar spots, b) Fitted regular hexagonal grid, c) Fitted irregular hexagonal grid, d) Identified vectors of contracting forces

Because the CellForce hardware was still under development, the image processing was tested on real images obtained by using a confocal laser scanning microscope (CLSM). The images of pillar matrix with cell cultures were registered and processed. The pillar matrix made of Sylgard and Elastollan with the different pillar surface coatings were used. The example results of image processing for human bone marrow cells are shown in Fig. 12. The pillar matrix is made of Sylgard with 10 MPa Young's modulus with 5 μm pillar diameter and 25 μm pillar height. The scale of 100 nN is drawn in the bottom left corner of the image. The arrows show detected deflection of the pillars but the deflections are very small comparing to the

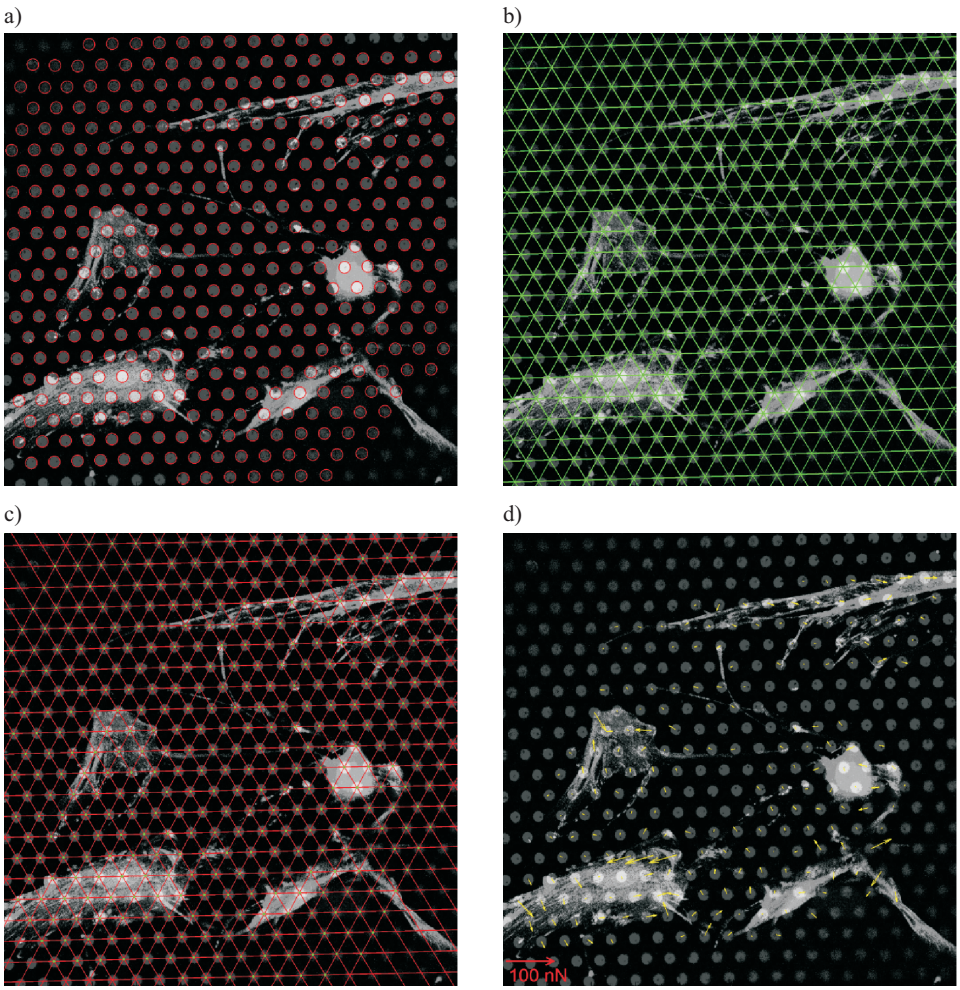

Fig. 12. Cell force identification for Sylgard pillar matrix (Young's modulus 10 MPa, pillar diameter 5 μm, pillar height 25 μm) with human bone marrow cells, a) Identified pillar spots, b) Fitted regular hexagonal grid, c) Fitted irregular hexagonal grid, d) Identified force vectors

simulation. The detected local forces do not form any regular system expected for the moving or contracting cells. There may be several reasons of a lack of detection of cell influence with the pillared substrate. The new experiments with new pillar materials and coatings will be continued.

5. Conclusions

The image analysis algorithm for a cell force measurement using a patterned substrate was elaborated and tested using simulated and real data. The algorithm is dedicated to a hexagonal structure of pillar matrix. The elaborated automatic procedure for reference hexagonal grid identification eliminates need of registering of additional reference images. It also eliminates need of recognition of cells in fluorescence images. The algorithm itself finds bent pillars and excludes them from calculating the reference grid. Additionally, the algorithm eliminates not only pillars covered by the cells but also the pillars deformed during the moulding process from calculations. The algorithm was positively verified with simulated data. The pillar bending can be detected using the elaborated algorithm. The processing toolbox was elaborated for image presentation, image processing, cell forces calculation and visualization. The first experiments were performed with living cells. Due to very small pillar deflection in the range of accuracy of the method the cell forces could not be determined. The algorithm will be used for new images obtained in next experiments with new pillar materials and new coatings.

Acknowledgments

The study was supported by the European Commission through the specific targeted research project Cell Force of the 6th FP (Contract N°: NMP4-CT-2005-016626).

References

1. Huang S., Ingber D.E.: The structural and mechanical complexity of cell-growth control. Nat. Cell Biol. 1999, 1, E131–E138.
2. Wong J.Y., Leach J.B., Brown X.Q.: Balance of chemistry, topography, and mechanics at the cell--biomaterial interface: issues and challenges for assessing the role of substrate mechanics on cell response. Surf. Sci. 2004, 570, 119–133.
3. Eastwood M., McGrouther D.A., Brown R.A.: A culture force monitor for measurement of contraction forces generated in human dermal fibroblast cultures: evidence for cell–matrix mechanical signalling. Biochim. Biophys. Acta 1994, 1201, 186–192.
4. Wrobel L.K., Fray T.R., Molloy J.E., Adams J.J., Armitage M.P., Sparrow J.C.: Contractility of single human dermal myofibroblasts and fibroblasts. Cell Motil Cytoskeleton 2002, 52, 82–90.
5. Harris A.K. Jr.: Tissue culture cells on deformable substrata: biomechanical implications. J. Biomech. Eng. 1984, 106, 1, 19–24.

6. Lo C.M., Wang H.B., Dembo M., Wang Y.L.: Cell movement is guided by the rigidity of the substrate. Biophys. J. 2000, 79, 144–152.
7. Galbraith C.G., Sheetz M.P.: A micromachined device provides a new bend on fibroblast traction forces. Cell Biology Proc. Natl. Acad. Sci. /USA/ 1997, 94, 9114–9118.
8. Tan J.L., Tien J., Pirone D.M., Gray D.S., Bhadriraju K., Chen C.S.: Cells lying on a bed of microneedles: An approach to isolate mechanical force. PNAS 2003, February 18, 100, 4, 1484–1489.
9. Lemon C.A., Sniadecki N.J., Ruiz S.A., Tan J.L., Romer L.H., Chen C.S.: Shear Force at the Cell--Matrix Interface: Enhanced Analysis for Microfabricated Post Array Detectors. Mech. Chem. Biosyst. 2005, 2, 1, 1–16.
10. Tanaka Y., Morishima K., Shimizu T., Kikuchi A., Yamato M., Okanobe T., Kitamori T: Demonstration of a PDMS-based bio-microactuator using cultured cardiomyocytes to drive polymer micropillars. Lab on a chip 2006, 6, 2, 230–235.
11. Yang M.T.: Geometric Considerations of Micro- to Nanoscale Elastomeric Post Arrays to Study Cellular Traction Forces. Adv. Mater. 2007, 19, 3119–3123.
12. Tymchenko N.: A Novel Cell Force Sensor for Quantification of Traction during Cell Spreading and Contact Guidance. Biophysical Journal 2007, 93, 1, 335–345.
13. Cesa CM, Kirchgeßner N, Mayer D, Schwarz US, Hoffmann B, Merkel R, Micropatterned silicone elastomer substrates for high resolution analysis of cellular force patterns. Review of Scientific Instruments 2007, 78, 3, 78, 034301.
14. Kaiser J.P., Bruinink A.: Investigating cell–material interactions by monitoring and analysing cell migration. Chemistry and Materials Science 2004, 15, 429–435.
15. Alves P., Coelho J.F.J., Haack J., Rota A., Bruinink A., Gil M.H.: Surface modification and characterization of thermoplastic polyurethane. European Polymer Journal 2009, 45, 5, 1412–1419.
16. Alves P., Kaiser J.P., Haack J., Salk N., Bruinink A., Sousa H.C., M.H. Gil1: Surface modification of thermoplastic polyurethane in order to enhance reactivity and avoid cell adhesion. Colloid and Polymer Science 2009, 287, 12, 1469–1474.
17. Ganz A., Lambert M., Saez A., Silberzan P., Buguin A., Mege R.M., Ladoux B.: Traction forces exerted through N-cadherin contacts. Biol. Cell 2006, 98, 721–730.
18. Zaidel-Bar R, Cohen M, Addadi L and Geiger B: Hierarchical assembly of cell-matrix adhesion complexes. Biochemical Society Transactions, 2004, 32(Pt3), 4160–4120
19. Salk N., Haack J., Kaiser J.P., Bruinink A., Rota A.: Biological sensor for cell monitoring via micro injection moulding technology, European Society for Precision Engineering and Nanotechnology. EUSPEN 2008. Vol.2: 10th Anniversary International Conference, Kongresshaus Zürich, 18th-22nd May 2008, ISBN: 978-0-9553082-5-3, 587–591.
20. Jain A.: Fundamentals of Digital Image Processing. Prentice-Hall 1989.